Hindawi
Wireless Communications and Mobile Computing
Volume 2018, Article ID 7178631, 6 pages
https://doi.org/10.1155/2018/7178631

Research Article

New 3D 16-Ary Signal Constellations and Their Symbol Error Probabilities in AWGN and Rayleigh Fading Channels

Zhenxing Chen,[1] Jiaheng Liu,[1] Shuang Li,[2] and Seog Geun Kang[3]

[1] *School of Mechanical Engineering and Electronic Information, China University of Geosciences, Wuhan, China*
[2] *Department of Electrical and Electronic Engineering, Gyeongsang National University, Jinju, Republic of Korea*
[3] *Department of Semiconductor Engineering and the Engineering Research Institute (ERI), Gyeongsang National University, Jinju, Republic of Korea*

Correspondence should be addressed to Seog Geun Kang; sgkang@gnu.ac.kr

Received 5 April 2018; Accepted 31 July 2018; Published 13 August 2018

Academic Editor: Donatella Darsena

Two three-dimensional (3D) 16-ary signal constellations having extended lattice structures are presented in this paper. The theoretical symbol error probabilities (SEPs) of the new constellations in additive white Gaussian noise (AWGN) and Rayleigh fading channel are derived. Computer simulation confirms that the closed-form expressions for average SEPs of the constellations in the AWGN channel are very accurate. The theoretical SEP upper bounds in the Rayleigh fading channel are very tight. Since the presented constellations have larger minimum Euclidean distance (MED) than the conventional one, error performance can be improved up to 0.9 dB in an AWGN environment. Hence, the proposed constellations and their theoretical analysis can be used as a reference for the development of a wireless communication system with 3D signal constellations.

1. Introduction

A signal constellation is one of the essential components to form a digital communication system. Recently, three-dimensional (3D) signal constellations have been studied widely in the fields of wireless communications and optical communications [1–8]. Some 3D constellations and their theoretical symbol error probabilities (SEPs) in additive white Gaussian noise (AWGN) channel have been introduced in [2–7]. Four vertices of the regular tetrahedron are reported as an optimal set of the 4-ary signal constellation. The typical structure for an 8-ary signal set is the regular hexahedron, and its twisted structure is also introduced to increase the minimum Euclidean distance (MED) among symbols [4, 5].

Designing a good multilevel 3D signal constellation under some limitations is a complicated issue. Repetitive search algorithms have been used to construct multilevel 3D constellations with constraints such as a constant amplitude and the maximized distance among symbols [1, 2]. As an example, the downhill simplex method generates a set of symbols that are located on the surface of a sphere and maximize the MED [2]. However, the repetitive algorithm cannot guarantee that the constellations generated are either regular or symmetric. Thus, they may not be suitable for practical implementation of a communication system. In [6], a simple method to design 3D signal constellation consisting of 32 or more symbols has been presented. Here, the multilevel constellations are created simply by extending the regular hexahedron in three dimensions. In addition, the constellations are perfectly symmetric with respect to the origin.

The 3D 16-ary constellations have also been studied in [2, 5, 7, 8]. In [2], Betti used the repetitive algorithm to compute the coordinates of 16-ary constellation which was optimum in the sense of the MED. Later, Chen [5] introduced another symbol set that had larger MED than Betti's work. Since a 16-ary phase shift keying (16-PSK) format was simply extended into 3D space, the former had much less computational load than the latter. In the meantime, the 3D 16-ary constellations based on the regular hexahedron were also presented in [7, 8]. They had a dual lattice configuration called cube-in-cube geometry. Since most of them have twisted structures, accurate SEP even in an AWGN channel has not been presented. Thus, theoretical error performance of the 16-ary constellations in the Rayleigh fading channel has never been reported yet.

In this paper, we present two 3D 16-ary signal constellations having extended lattice structures for future wireless communications. Although the presented constellations are not perfectly symmetric with respect to the origin, they have larger MEDs than the dual lattice configuration reported in [8]. We also compute the theoretical SEPs of the new constellations in an AWGN channel. In particular, the theoretical upper bounds of the error probability in the Rayleigh fading channel are derived for the first time. Simulation shows that the theoretical analysis on the SEP in the AWGN environment is accurate, and the SEP upper bounds in the Rayleigh fading channel are very tight.

The rest of this paper is as follows. In Section 2, the structures of new 3D 16-ary constellations are introduced. The theoretical error probabilities of the proposed constellations in AWGN and Rayleigh fading channels are derived in Section 3. And the results of computer simulation are presented and analyzed in Section 4. Finally, some concluding remarks are drawn in Section 5.

2. The New 3D 16-Ary Signal Constellations

Repetitive search algorithms such as the downhill simplex method have been exploited to compute the coordinates of symbols in the 3D signal space [1, 2]. One of the main concerns here is to maximize the MED among symbols. The 3D 16-ary constellations generated by the algorithm do not always have a suitable structure for application to a communication system.

In this paper, we consider a lattice structure obtained by extending the regular hexahedron for simple design and analysis. The new 16-ary constellations are shown in Figure 1. The configuration in Figure 1(a) named L_1 is an extended rectangular lattice. To reduce average power of the signal set, 2 outermost symbols (for example, N_1 and N_2) that are symmetric with respect to the origin among the 18 symbols are removed to form the L_2 constellation in Figure 1(b).

Consider that $S_k = (x, y, z)$, $k = 0, 1, \ldots, 15$, are symbols of a 3D signal constellation, where x, y, and z are the coordinates of a symbol in the 3D signal space. To transmit the 3D signals, the Gram-Schmidt orthogonalization procedure is usually exploited. Thus, the transmitted signal $s(t)$ can be represented as

$$s(t) = x\phi_x(t) + y\phi_y(t) + z\phi_z(t), \tag{1}$$

where $\phi_x(t)$, $\phi_y(t)$, and $\phi_z(t)$ are the orthogonal basis functions [6, 9]. Assume that the Euclidean distance among adjacent symbols is d. The symbol coordinates of the proposed constellations in Figure 1 can be represented as a 3×16 matrix form as follows:

$$\begin{gathered}
S_{L_1} = \begin{bmatrix} \frac{d}{2} & -\frac{d}{2} & -\frac{d}{2} & \frac{d}{2} & \frac{3d}{2} & -\frac{3d}{2} & -\frac{3d}{2} & \frac{3d}{2} & \frac{d}{2} & -\frac{d}{2} & -\frac{d}{2} & \frac{d}{2} & \frac{3d}{2} & -\frac{3d}{2} & -\frac{3d}{2} & \frac{3d}{2} \\ \frac{d}{2} & \frac{d}{2} & -\frac{d}{2} & -\frac{d}{2} & \frac{d}{2} & \frac{d}{2} & -\frac{d}{2} & -\frac{d}{2} & \frac{d}{2} & \frac{d}{2} & -\frac{d}{2} & -\frac{d}{2} & \frac{d}{2} & \frac{d}{2} & -\frac{d}{2} & -\frac{d}{2} \\ \frac{d}{2} & \frac{d}{2} & \frac{d}{2} & \frac{d}{2} & \frac{d}{2} & \frac{d}{2} & \frac{d}{2} & \frac{d}{2} & -\frac{d}{2} & -\frac{d}{2} & -\frac{d}{2} & -\frac{d}{2} & -\frac{d}{2} & -\frac{d}{2} & -\frac{d}{2} & -\frac{d}{2} \end{bmatrix}, \\
S_{L_2} = \begin{bmatrix} 0 & d & 0 & -d & 0 & d & -d & -d & 0 & d & 0 & -d & 0 & d & -d & -d \\ 0 & 0 & d & 0 & -d & -d & d & -d & 0 & 0 & d & 0 & -d & -d & d & -d \\ \frac{d}{2} & \frac{d}{2} & \frac{d}{2} & \frac{d}{2} & \frac{d}{2} & \frac{d}{2} & \frac{d}{2} & \frac{d}{2} & -\frac{d}{2} & -\frac{d}{2} & -\frac{d}{2} & -\frac{d}{2} & -\frac{d}{2} & -\frac{d}{2} & -\frac{d}{2} & -\frac{d}{2} \end{bmatrix}.
\end{gathered} \tag{2}$$

Then the average powers of both constellations are computed as

$$\begin{aligned}
E_{s,L_1} &= \frac{8}{16}\left[\left(\frac{d}{2}\right)^2 + \left(\frac{d}{2}\right)^2 + \left(\frac{d}{2}\right)^2\right] \\
&\quad + \frac{8}{16}\left[\left(\frac{3d}{2}\right)^2 + \left(\frac{d}{2}\right)^2 + \left(\frac{d}{2}\right)^2\right] = \frac{7}{4}d^2, \\
E_{s,L_2} &= \frac{2}{16}\left[0 + 0 + \left(\frac{d}{2}\right)^2\right] + \frac{8}{16}\left[d^2 + 0 + \left(\frac{d}{2}\right)^2\right] \\
&\quad + \frac{6}{16}\left[d^2 + d^2 + \left(\frac{d}{2}\right)^2\right] = \frac{3}{2}d^2,
\end{aligned} \tag{3}$$

respectively.

3. The Theoretical SEPs of the Presented Constellations

In an AWGN environment, the received signal is $r(t) = s(t) + n(t)$, where

$$n(t) = n_x\phi_x(t) + n_y\phi_y(t) + n_z\phi_z(t) \tag{4}$$

is a Gaussian random process. n_x, n_y, and n_z are independent and identically distributed Gaussian random variables with zero-mean and variance of σ^2. Thus, the probability density function (PDF) of the received signals is

$$P(x, y, z) = \frac{1}{(2\pi\sigma^2)^{3/2}} e^{-((x-\mu_x)^2+(y-\mu_y)^2+(z-\mu_z)^2)/2\sigma^2}, \tag{5}$$

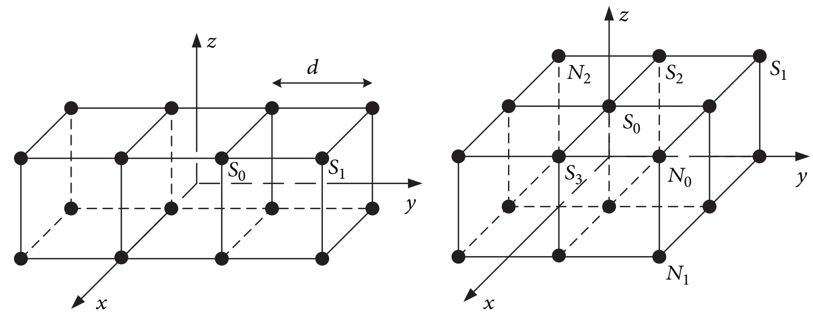

(a) (b)

Figure 1: The new 3D 16-ary signal constellations (a) L_1, (b) L_2.

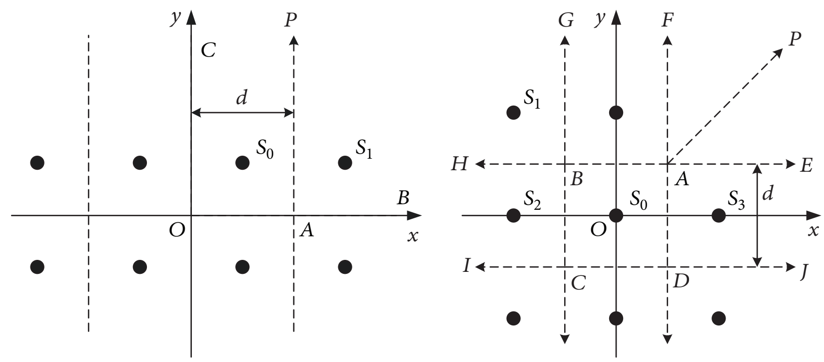

(a) (b)

Figure 2: The xy plane projection of the decision regions (a) L_1, (b) L_2.

where μ_x, μ_y, and μ_z are the mean values of 3D components. In general, correct decision of a symbol is made when the recovered symbol falls inside the corresponding decision region. Thus, the probability of correct decision for a symbol can be computed as

$$P_c = p(x_1 < x < x_2)\, p(y_1 < y < y_2)\, p(z_1 < z < z_2), \quad (6)$$

where x_1, x_2, y_1, y_2, z_1, and z_2 are decision boundaries for a symbol. As the constellations in Figure 1 are symmetric, the projection of the decision regions on the xy plane shown in Figure 2 can be used to compute the probability of correct decision. A pair of the outermost points represented as N_1 and N_2 in Figure 1(b) is not included in Figure 2 because they are not the elements of L_2 constellation.

3.1. AWGN Channel. For L_1 constellation, the probabilities of correct decision of $S_0 = (d/2, d/2, d/2)$ and $S_1 = (3d/2, d/2, d/2)$ with the decision region $COAP$ and PAB in Figure 2(a), respectively, can be calculated as

$$\begin{aligned} P_{c_0,L_1} &= p(0 < x < d)\, p(0 < y < \infty)\, p(0 < z < \infty) \\ &= (1-2q)(1-q)^2, \\ P_{c_1,L_1} &= p(d < x < \infty)\, p(0 < y < \infty)\, p(0 < z < \infty) \\ &= (1-q)^3, \end{aligned} \quad (7)$$

where $q = Q(d/2\sigma)$. $Q(\cdot)$ is the Gaussian Q-function [9]. According to (7), the average SEP of L_1 can be computed as

$$\begin{aligned} P_{L_1}(\gamma_s) &= 1 - \frac{1}{16}\left(8P_{c_0,L_1} + 8P_{c_1,L_1}\right) = \frac{7}{2}q - 4q^2 + \frac{3}{2}q^3 \\ &= \frac{7}{2}Q\left(\sqrt{\frac{2}{7}\gamma_s}\right) - 4Q^2\left(\sqrt{\frac{2}{7}\gamma_s}\right) \\ &\quad + \frac{3}{2}Q^3\left(\sqrt{\frac{2}{7}\gamma_s}\right), \end{aligned} \quad (8)$$

where $\gamma_s = E_{s,L_1}/N_0$ represents signal-to-noise ratio (SNR). $N_0 = 2\sigma^2$ is the single-sided power spectral density of the AWGN channel.

In Figure 2(b), the decision regions of $S_0 = (0, 0, d/2)$, $S_1 = (-d, d, d/2)$, and $S_2 = (-d, 0, d/2)$ are $ABCD$, GBH, and $HBCI$, respectively. Thus, the correct decision probabilities of S_0, S_1, and S_2 are given as

$$\begin{aligned} P_{c_0,L_2} &= p\left(-\frac{d}{2} < x < \frac{d}{2}\right) p\left(-\frac{d}{2} < y < \frac{d}{2}\right) \\ &\quad \cdot p(0 < z < \infty) = (1-q)(1-2q)^2, \\ P_{c_1,L_2} &= p\left(-\infty < x < -\frac{d}{2}\right) p\left(\frac{d}{2} < y < \infty\right) \\ &\quad \cdot p(0 < z < \infty) = (1-q)^3, \end{aligned}$$

$$P_{c_2,L_2} = p\left(-\infty < x < -\frac{d}{2}\right) p\left(-\frac{d}{2} < y < \frac{d}{2}\right) \cdot p(0 < z < \infty) = (1-2q)(1-q)^2, \tag{9}$$

respectively. The decision region of $S_3 = (d, 0, d/2)$ is $PADJ$ which is equivalent to $EADJ + FAE/2$. Since the probability of $EADJ$ is the same as P_{c_2,L_2} in (9), the correct decision probability of S_3 is

$$P_{c_3,L_2} = P_{c_2,L_2} + \frac{1}{2} p\left(\frac{d}{2} < x < \infty\right) p\left(\frac{d}{2} < y < \infty\right) \cdot p(0 < z < \infty) = \left(1 - \frac{3}{2}q\right)(1-q)^2. \tag{10}$$

Thus, the theoretical SEP of L_2 constellation is computed as

$$\begin{aligned} P_{L_2}(\gamma_s) &= 1 - \frac{1}{16}\left(2P_{c_0,L_2} + 6P_{c_1,L_2} + 4P_{c_2,L_2} + 4P_{c_3,L_2}\right) \\ &= \frac{29}{8}q - \frac{35}{8}q^2 + \frac{7}{4}q^3 \\ &= \frac{29}{8}Q\left(\sqrt{\frac{1}{3}\gamma_s}\right) - \frac{35}{8}Q^2\left(\sqrt{\frac{1}{3}\gamma_s}\right) \\ &\quad + \frac{7}{4}Q^3\left(\sqrt{\frac{1}{3}\gamma_s}\right). \end{aligned} \tag{11}$$

3.2. Rayleigh Fading Channel. In a Rayleigh fading channel, as it is well known, SNR is a random variable with PDF $f_R(\gamma_s) = (1/\Lambda)\exp(-\gamma_s/\Lambda)$, where Λ is the average SNR per symbol. Then the average SEP can be calculated by integrating the error probability in AWGN over fading distribution [10] as follows:

$$P_R(\Lambda) = \int_0^\infty f_R(\gamma_s) P(\gamma_s)\, d\gamma_s. \tag{12}$$

Hence, the average SEP of the constellation in Figure 1(a) over Rayleigh fading channel is

$$\begin{aligned} P'_{L_1}(\Lambda) &= \int_0^\infty f_R(\gamma_s) P_{L_1}(\gamma_s)\, d\gamma_s \\ &= \frac{7}{2}\int_0^\infty \frac{1}{\Lambda}e^{-\gamma_s/\Lambda} Q\left(\sqrt{\frac{2}{7}\gamma_s}\right) d\gamma_s \\ &\quad - 4\int_0^\infty \frac{1}{\Lambda}e^{-\gamma_s/\Lambda} Q^2\left(\sqrt{\frac{2}{7}\gamma_s}\right) d\gamma_s \\ &\quad + \frac{3}{2}\int_0^\infty \frac{1}{\Lambda}e^{-\gamma_s/\Lambda} Q^3\left(\sqrt{\frac{2}{7}\gamma_s}\right) d\gamma_s. \end{aligned} \tag{13}$$

The integral of the first term of the right-hand side of (13) can be calculated as

$$\begin{aligned} &\int_0^\infty \frac{1}{\Lambda}e^{-\gamma_s/\Lambda} Q\left(\sqrt{\frac{2}{7}\gamma_s}\right) d\gamma_s \\ &= \int_0^{\pi/2}\int_0^\infty \frac{1}{\pi\Lambda} e^{-(1/\Lambda + 1/7\sin^2\theta)\gamma_s} d\gamma_s d\theta \\ &= \frac{1}{\pi}\int_0^{\pi/2} \frac{7\sin^2\theta}{\Lambda + 7\sin^2\theta} d\theta = \frac{1}{2} - \frac{1}{2}\sqrt{\frac{\Lambda}{\Lambda+7}}, \end{aligned} \tag{14}$$

where Q-function is replaced by an integral of the equivalent trigonometric function when the variable $v > 0$ [11], that is,

$$Q(v) = \frac{1}{\pi}\int_0^{\pi/2} e^{-v^2/2\sin^2\theta} d\theta. \tag{15}$$

And the integral equation defined in [12] is exploited.

An equivalent form of $Q^2(v)$ [13] is

$$Q^2(v) = \frac{1}{\pi}\int_0^{\pi/4} e^{-v^2/2\sin^2\theta} d\theta. \tag{16}$$

Applying (16) to the second integral in (13), we have

$$\begin{aligned} &\int_0^\infty \frac{1}{\Lambda}e^{-\gamma_s/\Lambda} Q^2\left(\sqrt{\frac{2}{7}\gamma_s}\right) d\gamma_s \\ &= \int_0^{\pi/4}\int_0^\infty \frac{1}{\pi\Lambda} e^{-(1/\Lambda + 1/7\sin^2\theta)\gamma_s} d\gamma_s d\theta \\ &= \frac{1}{\pi}\int_0^{\pi/4} \frac{7\sin^2\theta}{\Lambda + 7\sin^2\theta} d\theta \\ &= \frac{1}{4} - \frac{1}{\pi}\sqrt{\frac{\Lambda}{\Lambda+7}}\tan^{-1}\left(\sqrt{\frac{\Lambda+7}{\Lambda}}\right). \end{aligned} \tag{17}$$

A trigonometric function equivalent to $Q^3(v)$ in (13) is too complex to calculate an exact expression [14]. To compute the last integral term in (13), we use the Chernoff bound of $Q(v) \le (1/2)\exp(-v^2/2)$. Then an upper bound of the third integral in (13) can be obtained as follows:

$$\begin{aligned} &\int_0^\infty \frac{1}{\Lambda}e^{-\gamma_s/\Lambda} Q^3\left(\sqrt{\frac{2}{7}\gamma_s}\right) d\gamma_s \\ &\le \int_0^\infty \frac{1}{\Lambda}e^{-\gamma_s/\Lambda}\left(\frac{1}{2}e^{-\gamma_s/7}\right)^3 d\gamma_s = \frac{7}{8(3\Lambda+7)}. \end{aligned} \tag{18}$$

Hence, the average SEP in (13) is bounded as

$$\begin{aligned} P'_{L_1}(\Lambda) &\le \frac{7}{2}\left(\frac{1}{2} - \frac{1}{2}\sqrt{\frac{\Lambda}{\Lambda+7}}\right) \\ &\quad - 4\left[\frac{1}{4} - \frac{1}{\pi}\sqrt{\frac{\Lambda}{\Lambda+7}}\tan^{-1}\left(\sqrt{\frac{\Lambda+7}{\Lambda}}\right)\right] \\ &\quad + \frac{3}{2}\left[\frac{7}{8(3\Lambda+7)}\right] \\ &= \frac{3}{4} + \frac{21}{16(3\Lambda+7)} - \frac{7}{4}\sqrt{\frac{\Lambda}{\Lambda+7}} \\ &\quad + \frac{4}{\pi}\sqrt{\frac{\Lambda}{\Lambda+7}}\tan^{-1}\left(\sqrt{\frac{\Lambda+7}{\Lambda}}\right). \end{aligned} \tag{19}$$

In the case of L_2 constellation, the average SEP over Rayleigh fading channel can be computed as

$$\begin{aligned} P'_{L_2}(\Lambda) &= \int_0^\infty f_R(\gamma_s) P_{L_2}(\gamma_s)\, d\gamma_s \\ &= \frac{29}{8}\int_0^\infty \frac{1}{\Lambda} e^{-\gamma_s/\Lambda} Q\left(\sqrt{\frac{1}{3}\gamma_s}\right) d\gamma_s \\ &\quad - \frac{35}{8}\int_0^\infty \frac{1}{\Lambda} e^{-\gamma_s/\Lambda} Q^2\left(\sqrt{\frac{1}{3}\gamma_s}\right) d\gamma_s \\ &\quad + \frac{7}{4}\int_0^\infty \frac{1}{\Lambda} e^{-\gamma_s/\Lambda} Q^3\left(\sqrt{\frac{1}{3}\gamma_s}\right) d\gamma_s. \end{aligned} \tag{20}$$

Referring to the calculation processes of (14), (17), and (18), the integral terms in (20) can be computed as

$$\begin{aligned} &\int_0^\infty \frac{1}{\Lambda} e^{-\gamma_s/\Lambda} Q\left(\sqrt{\frac{1}{3}\gamma_s}\right) d\gamma_s = \frac{1}{2} - \frac{1}{2}\sqrt{\frac{\Lambda}{\Lambda+6}}, \\ &\int_0^\infty \frac{1}{\Lambda} e^{-\gamma_s/\Lambda} Q^2\left(\sqrt{\frac{1}{3}\gamma_s}\right) d\gamma_s \\ &\quad = \frac{1}{4} - \left[\frac{1}{\pi}\sqrt{\frac{\Lambda}{\Lambda+6}} \tan^{-1}\left(\sqrt{\frac{\Lambda+6}{\Lambda}}\right)\right], \\ &\int_0^\infty \frac{1}{\Lambda} e^{-\gamma_s/\Lambda} Q^3\left(\sqrt{\frac{1}{3}\gamma_s}\right) d\gamma_s \le \frac{1}{4(\Lambda+2)}. \end{aligned} \tag{21}$$

Thus, the theoretical upper bound of the average SEP in (20) can be represented as

$$\begin{aligned} P'_{L_2}(\Lambda) &\le \frac{29}{8}\left(\frac{1}{2} - \frac{1}{2}\sqrt{\frac{\Lambda}{\Lambda+6}}\right) \\ &\quad - \frac{35}{8}\left[\frac{1}{4} - \frac{1}{\pi}\sqrt{\frac{\Lambda}{\Lambda+6}} \tan^{-1}\left(\sqrt{\frac{\Lambda+6}{\Lambda}}\right)\right] \\ &\quad + \frac{7}{4}\left[\frac{1}{4(\Lambda+2)}\right] \\ &= \frac{23}{32} + \frac{7}{16(\Lambda+2)} - \frac{29}{16}\sqrt{\frac{\Lambda}{\Lambda+6}} \\ &\quad + \frac{35}{8\pi}\sqrt{\frac{\Lambda}{\Lambda+6}} \tan^{-1}\left(\sqrt{\frac{\Lambda+6}{\Lambda}}\right). \end{aligned} \tag{22}$$

4. Performance Analysis

The MED of a constellation is one of the key parameters determining error performance of a communication system. The MEDs of the presented 3D 16-ary constellations are compared with Cho's constellation [8] in Table 1. Here, all constellations are normalized to have the average power of unity. Table 1 shows that the MED of L_2 constellation is increased about 10.6% as compared with Cho's one.

To verify the theoretical SEP of the presented constellations in AWGN and Rayleigh fading channels, computer simulation has been carried out. Exploiting the MATLAB which is well-known simulation software, the 3D transmission system and both channel models are designed. 10^8 3D symbols are transmitted by the form of (1), where the mathematical model of the orthogonal basis functions in a vector form is $\phi_x(t) = \left[1/\sqrt{3}\;\; 0\;\; 0\right]^T$, $\phi_y(t) = \left[0\;\; 1/\sqrt{3}\;\; 0\right]^T$, $\phi_z(t) = \left[0\;\; 0\;\; 1/\sqrt{3}\right]^T$ for $0 \le t < T_s$, respectively, where T_s is the symbol duration [9]. The simulation results are plotted in Figure 3. It can be observed that the theoretical SEPs of the presented constellations in the AWGN channel match exactly the simulation results. Hence, the SEP expressions in (8) and (11) seem to be accurate. When the L_1 constellation is exploited, the system has almost the same error performance reported in [8]. In the case of L_2 constellation, the SEP is improved about 0.9 dB as compared with Cho's constellation at the SEP of 10^{-6}. Such performance gain is attributed to the increased MED of the L_2 constellation.

In Figure 3, we also present the theoretical SEPs of the proposed constellations and simulation results in the Rayleigh fading channel. The error performance obtained by computer simulation is very tightly bounded by the theoretical SEP upper bounds derived in (19) and (22). Especially when the average SNR is larger than 15 dB, two performance curves are almost the same.

Table 1: The MEDs of the presented constellations.

Constellation	MED	Increment
Cho's	0.7385	
L_1	0.7559	2.4%
L_2	0.8165	10.6%

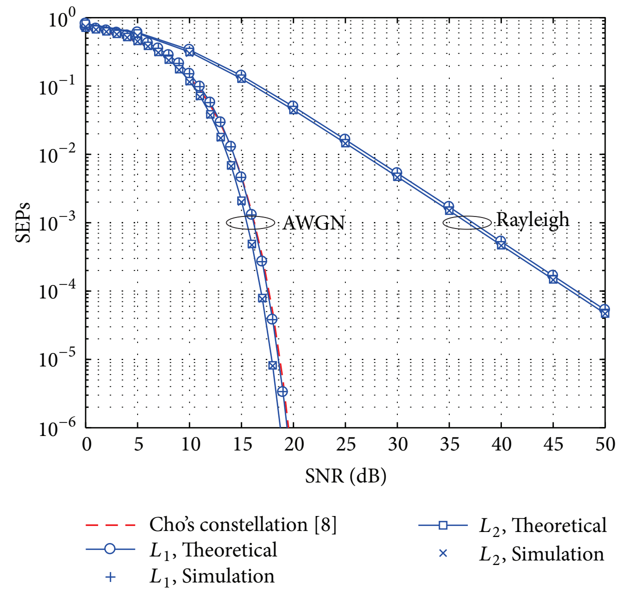

Figure 3: SEPs of the 3D 16-ary signal constellations.

5. Conclusions

Two 3D 16-ary signal constellations with extended lattice structures are introduced in this paper. In addition, their theoretical SEPs both in AWGN and Rayleigh fading channel are presented. Simulation confirms that the theoretical SEPs in the AWGN channel and SEP upper bounds in the Rayleigh fading channel are very accurate. Due to the increased MED, the new constellations provide better error performance than the conventional one. In addition, since the constellations introduced in this paper have an extended configuration of the regular hexahedron, they are much more practical than the previous ones. The proposed constellations and their exact SEPs derived can be applied for future development of wireless or optical communication systems with 3D constellations.

Data Availability

The data used to support the findings of this study are available from the corresponding author upon request.

Conflicts of Interest

The authors declare that there are no conflicts of interest regarding the publication of this paper.

Acknowledgments

The work carried out by Z. Chen has been supported by the National Natural Science Foundation of China (NSFC) (61401409 and 61771436) and Fundamental Research Funds for the Central Universities (China University of Geosciences (Wuhan), CUGL170211). Seog Geun Kang is supported by the Basic Science Research Program through the National Research Foundation of Korea (NRF) funded by the Ministry of Education (2015R1D1A1A01060057).

References

[1] J.-E. Porath and T. Aulin, "Design of multidimensional signal constellations," *IEE Proceedings Communications*, vol. 150, no. 5, pp. 317–323, 2003.

[2] S. Betti, G. De Marchis, and E. Iannone, "Polarization modulated direct detection optical transmission systems," *Journal of Lightwave Technology*, vol. 10, no. 12, pp. 1985–1997, 1992.

[3] M. Khabbazian, J. Hossain, M.-S. Alouini, and V. K. Bhargava, "Exact method for the error probability calculation of three-dimensional signal constellations," *IEEE Transactions on Communications*, vol. 57, no. 4, pp. 922–925, 2009.

[4] Z. Chen, E. C. Choi, and S. G. Kang, "Closed-form expressions for the symbol error probability of 3-D OFDM," *IEEE Communications Letters*, vol. 14, no. 2, pp. 112–114, 2010.

[5] Z. Chen and S. G. Kang, "Three-dimensional modulation formats with constant power for optical communications," *Optics Express*, vol. 19, no. 23, pp. 22358–22363, 2011.

[6] S. G. Kang, Z. Chen, J. Y. Kim, J. S. Bae, and J.-S. Lim, "Construction of higher-level 3-D signal constellations and their accurate symbol error probabilities in AWGN," *IEEE Transactions on Signal Processing*, vol. 59, no. 12, pp. 6267–6272, 2011.

[7] Z. Chen and S. G. Kang, "Probability of symbol error of OFDM system with 3-dimensional signal constellations," in *Proceedings of the International Symposium on Consumer Electronics*, pp. 442–446, Kyoto, Japan, May 2009.

[8] S. Cho and S. K. Park, "Improved 16-ary constellation mapping for three-dimensional OFDM systems," *IEEE Electronics Letters*, vol. 48, no. 9, pp. 530–532, 2012.

[9] J. G. Proakis and S. Salehi, *Digital Communications*, McGraw-Hill, Singapore, 5th edition, 2008.

[10] X. Dong and N. C. Beaulieu, "New analytical probability of error expressions for classes of orthogonal signals in Rayleigh fading," *IEEE Transactions on Communications*, vol. 51, no. 6, pp. 849–853, 2003.

[11] J. Craig, "A new, simple and exact result for calculating the probability of error for two-dimensional signal constellations," in *Proceedings of the IEEE Conference (MILCOM '91)*, pp. 25.5.1–25.5.5, Boston, MA, USA, November 1991.

[12] I. S. Gradshteyn and I. M. Ryzhik, *Table of Integrals Series, and Products*, Academic Press: Elsevier, San Diego, Calif, USA, 8th edition, 2015.

[13] M. K. Simon, "Some new twists to problems involving the gaussian probability integral," *IEEE Transactions on Communications*, vol. 46, no. 2, pp. 200–210, 1998.

[14] M. K. Simon, "Single integral representations of certain integer powers of the Gaussian Q-function and their application," *IEEE Communications Letters*, vol. 6, no. 12, pp. 532–534, 2002.

Journal of Engineering
The Scientific World Journal
International Journal of Rotating Machinery
Journal of Sensors
Advances in Multimedia
Advances in Civil Engineering
Journal of Control Science and Engineering
Hindawi
Submit your manuscripts at
www.hindawi.com
Journal of Robotics
Journal of Electrical and Computer Engineering
Advances in OptoElectronics
VLSI Design
International Journal of Navigation and Observation
Modelling & Simulation in Engineering
International Journal of Aerospace Engineering
International Journal of Chemical Engineering
International Journal of Antennas and Propagation
Active and Passive Electronic Components
Shock and Vibration
Advances in Acoustics and Vibration